GAMOW–TELLER EXCITATIONS STUDIED BY WEAK AND STRONG INTERACTIONS*

Y. Fujita[a,b], B. Rubio[c], T. Adachi[a], B. Blank[d], H. Fujita[a]
W. Gelletly[e], F. Molina[c], S.E.A. Orrigo[c]

[a]Research Center for Nuclear Physics, Osaka University
Ibaraki, Osaka 567-0047, Japan
[b]Department of Physics, Osaka University, Toyonaka, Osaka 560-0043, Japan
[c]IFIC, CSIC-Universidad de Valencia, 46071 Valencia, Spain
[d]Centre d'Etudes Nucléaires de Bordeaux Gradignan, Université Bordeaux 1
UMR 5797 CNRS/IN2P3, BP 120, 33175 Gradignan, France
[e]Department of Physics, University of Surrey, Guildford GU2 7XH, Surrey, UK

(Received March 23, 2015)

Studying weak nuclear responses, especially the Gamow–Teller (GT) transitions starting from stable as well as unstable nuclei, provide crucial and critical information on nuclear structure. Therefore, the study of GT transitions is a key issue in nuclear physics and also nuclear-astrophysics. Under the assumption of isospin symmetry, it is expected that the structure of mirror nuclei and the GT transitions starting from their ground states are identical. We have studied the corresponding GT transitions starting from $T_z = \pm 1$ and ± 2 pf-shell nuclei, respectively, by means of hadronic $(^3\mathrm{He}, t)$ charge-exchange reactions and mirror β decays. The results on GT strength distributions measured in β decays and $(^3\mathrm{He}, t)$ reactions performed at an intermediate incident energy of 140 MeV/nucleon and 0° are compared. The combined results help provide an understanding of nuclear structure of nuclei far-from-stability.

DOI:10.5506/APhysPolB.46.657
PACS numbers: 21.10.Hw, 23.40.–s, 25.55.Kr, 27.40.+z

1. Introduction

Gamow–Teller (GT) transitions governed by the simple $\sigma\tau$ operator, where σ is the spin operator and τ is the isospin operator, represent the most common weak interaction processes of charged-current type [1]. They are of interest not only in nuclear structure physics, that we discuss here, but also in nuclear-astrophysics; they play crucial roles in various processes of nucleosynthesis [2].

* Presented at the Zakopane Conference on Nuclear Physics "Extremes of the Nuclear Landscape", Zakopane, Poland, August 31–September 7, 2014.

The main features of GT transitions can be summarized as follows [3]:

(1) They start from a nucleus with Z and N and lead to states in a neighboring nucleus with $Z \pm 1$ and $N \mp 1$. Thus the β^+-type GT transitions have the nature of $\Delta T_z = +1$ and the β^--type GT transitions $\Delta T_z = -1$, where T_z is defined by $(N - Z)/2$ and is the z component of the isospin T. As a result, they are of isovector (IV) nature with $\Delta \boldsymbol{T} = 1$ ($\Delta T = \pm 1$ or 0). Since GT transitions involve $\Delta \boldsymbol{S} = 1$ and $\Delta \boldsymbol{L} = 0$, they also have $\Delta \boldsymbol{J} = 1$ ($\Delta J = \pm 1$ or 0) and no parity change.

(2) They can be studied either in β decay (caused by weak interaction) or in Charge Exchange (CE) reactions (caused by strong interaction).

(3) Since the $\sigma\tau$ operator has no spatial component, transitions between states with similar spatial shapes are favored.

(4) In a simple, independent particle picture where the individual nucleons are in an orbit with orbital angular momentum ℓ and spin s, a GT transition connects initial and final states with the same ℓ. Therefore, the transitions are among the spin–orbit partners, *i.e.*, the $j_>$ $(= \ell + 1/2)$ and the $j_<$ $(= \ell - 1/2)$ orbits. The $j_> \leftrightarrow j_<$ transition and the transitions between the same orbits (*i.e.*, $j_> \leftrightarrow j_>$ and $j_< \leftrightarrow j_<$) are separated, in first order, by 3 to 6 MeV, the separation in energy of the spin–orbit partners.

(5) In contrast to the Fermi transitions, where only the T_z is changed by the τ operator and hence only a single state [the Isobaric Analog State (IAS)] is populated in the final nucleus, GT transitions involve both the σ and the τ operators and a variety of states can be populated. As a result, one can extract valuable structure information of the final nucleus.

(6) Besides the information on nuclear structure, GT transitions are also important in the understanding of many processes in nuclear astrophysics.

The most common transitions in β decay are the allowed Fermi and GT transitions governed by the τ and $\sigma\tau$ operators, respectively. The β decay provides direct access to the absolute GT transition strengths $B(\mathrm{GT})$ from the study of partial half-lives, Q_β-values and branching ratios [4]. We see that the inverse of the partial half-life, that shows how fast specific GT or Fermi transitions are, is proportional to the $B(\mathrm{GT})$ or $B(\mathrm{F})$ values,

$$1/t_j^{\mathrm{GT}} = (1/K)\lambda^2 f_j B_j(\mathrm{GT}) \tag{1}$$

for the j^{th} GT transition and

$$1/t^{\text{F}} = (1/K) f_{\text{F}} B(\text{F}) \,, \tag{2}$$

for the Fermi transition, where K is 6143.6(17) [5] and $\lambda = g_A/g_V = -1.270(3)$ [6]. The phase-space factors (f-factors) f_j and f_{F} are for the j^{th} GT transition and the Fermi transition, respectively, and are calculated from the Q_β value of each state. However, direct studies by means of weak processes give relatively limited information about GT transitions and the states excited via GT transitions (GT states); β decay can only access states at excitation energies lower than the decay Q-value, and neutrino-induced reactions have very small cross sections.

In contrast, charge-exchange (CE) reactions, such as the (p, n) or (^{3}He,t) reactions at intermediate beam energies and 0°, can selectively excite GT states up to high excitation energies in the final nucleus. In (p, n) reactions performed in the 1980s, it was found that at intermediate incoming energies of more than 100 MeV/nucleon, the reaction mechanism becomes simple and the $\sigma\tau$ part of the effective interaction becomes dominant. As a result, at momentum transfer $q = 0$, there is a close proportionality between the cross sections and the B(GT) values

$$\sigma^{\text{GT}}(0) \simeq \hat{\sigma}^{\text{GT}}(0) B(\text{GT}) \,, \tag{3}$$

where $\hat{\sigma}_{\text{GT}}(0)$ is a unit cross section for the GT transition at the momentum transfer $q = 0$ ($\approx 0°$). This close proportionality was first established in (p, n) reactions at intermediate energies of 120–200 MeV [7] and also examined in the (^{3}He, t) reaction [3, 8, 9]. Although there are exceptions, the B(GT) values, if they are not too small, usually agree well ($\approx 5\%$) with the B(GT) values observed in mirror β decays by applying only one normalization parameter [3]. A similar relationship is valid for the Fermi transitions [3].

In recent (^{3}He, t) measurements performed at RCNP, Osaka [10], energy resolutions of $\approx$ 30 keV have been achieved. This is an improvement of about one order-of-magnitude compared to the pioneering (p, n) reactions. As a result, it became possible to identify one-to-one correspondence of GT transitions studied in CE reactions and β decays and thus a detailed comparison of them is now possible [3]. In this paper, we discuss the combined analysis of the $T_z = \pm 1 \rightarrow 0$ and further $T_z = \pm 2 \rightarrow \pm 1$ GT transitions that can be studied in CE reaction and β-decay, respectively.

2. Study of $T_z = \pm 1$ mirror transitions

We have been studying $T_z = \pm 1 \rightarrow 0$ isospin analogous GT transitions starting from the 0^+ ground states of the even–even pf-shell nuclei. In these

transitions, the identical final 1^+ excited states are reached. The isospin symmetry in the $T_z = \pm 1 \rightarrow 0$ GT transitions is shown schematically in Fig. 1 for the $A = 50$ and 54 systems. In these A systems, the ground states of the $T_z = 0$ nuclei ^{50}Mn and ^{54}Co are the IAS of neighboring $T_z = \pm 1$ nuclei.

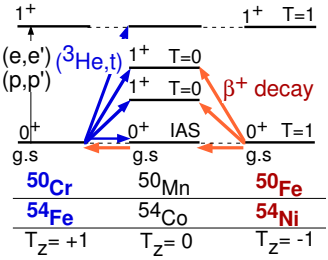

Fig. 1. (Color online) Schematic illustration of the "isospin symmetry" of GT transitions in the "$T = 1$ systems" with mass $A = 50$ and 54. The Coulomb displacement energies have been removed. The analogous $T_z = \pm 1 \rightarrow 0$ transitions can be studied by the $(^3\mathrm{He}, t)$ reaction and β decay, respectively, for the pf-shell nuclei. In these A systems, ground states are all analog states and have $T = 1$.

The $T_z = +1 \rightarrow 0$ transitions have been thoroughly studied using $(^3\mathrm{He}, t)$ reactions on the stable $T_z = +1$, even–even f-shell target nuclei ^{42}Ca [11], ^{46}Ti [12], ^{50}Cr [13], ^{54}Fe [14], and ^{58}Ni [15] [see Fig. 2 (b) for the 0° spectrum obtained in the ^{54}Fe$(^3\mathrm{He}, t)$ reaction].

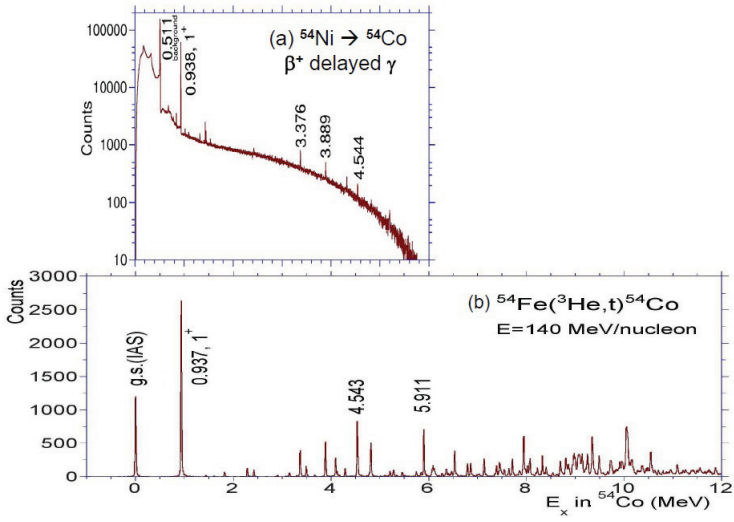

Fig. 2. (Color online) (a) The delayed-γ spectrum from the RISING array at GSI for the study of ^{54}Ni β decay. (b) The ^{54}Fe$(^3\mathrm{He}, t)^{54}$Co spectrum for events with scattering angles $\Theta \leq 0.5°$. The γ-ray peaks and CE-reaction peaks are seen at corresponding energies.

The corresponding $T_z = -1 \rightarrow 0$ β decays were studied for the unstable mirror nuclei ^{42}Ti, ^{46}Cr, ^{50}Fe, and ^{54}Ni produced at the fragment separator facility FRS at GSI [16]. The proton separation energies in the daughter $T_z = 0$ nuclei ^{42}Sc, ^{46}V, ^{50}Mn, and ^{54}Co are relatively large ($\approx$ 4–5 MeV). Therefore, the measurements of delayed-γ decay are essential for the derivation of branching ratios in these β-decay studies.

The measurements were performed using the RISING set-up consisting of 15 Euroball Cluster Ge detectors surrounding the DSSSD detectors. The DSSSDs were used for the detection of the implanted ions and the following β particles. As one can see from the delayed γ-ray spectrum obtained in the ^{54}Ni β-decay measurement [see Fig. 2 (a)], for strong γ-ray peaks corresponding CE-reaction peaks are observed at the same energies, suggesting a good mirror symmetry for the $T_z = \pm 1 \rightarrow 0$ GT transitions. GT transition strengths B(GT) were derived from the obtained high precision β-decay half-lives, excitation energies and β branching ratios.

These improved studies of $T_z = -1 \rightarrow 0$ β decays allowed a detailed comparison of the B(GT) values with those from the $T_z = +1 \rightarrow 0$ GT transitions derived from high-resolution $(^3\mathrm{He}, t)$ reactions on mirror target nuclei. Looking at the individual transitions obtained in both experiments, one finds some differences especially for weak transitions. However, the cumulative sums of the B(GT) distributions were very similar in the low-energy region (up to E_x = 4–5 MeV) where the direct comparison of these two studies was possible [16]. Then the knowledge of the B(GT) distributions could be extended up to higher excitation energies by the $(^3\mathrm{He}, t)$ reactions. Therefore, one can obtain an overall picture of the "absolute" B(GT) strengths for the "full range" of excitation energies that can be reached in $(^3\mathrm{He}, t)$ CE reactions using the β-decay B(GT) values as standards.

The B(GT) strength distribution obtained in the $^{54}\mathrm{Fe}(^3\mathrm{He}, t)^{54}\mathrm{Co}$ reaction [14] is shown up to E_x = 12 MeV in Fig. 3 (a) and compared with the result of the shell-model (SM) calculation using the GXPF1 interaction [17] shown in Fig. 3 (b), where a quenching factor of $(0.74)^2$ is included in the calculation. The experimental results show that the main part of the GT strength is in the GT Resonance (GTR) region of $E_x = 7 - -12$ MeV and the SM calculation could reproduce the concentration of the GT strength in this region. However, we see from the cumulative sums of the GT strengths shown in Fig. 3 (c) that the SM calculation overestimates the GT strength in the GTR region (for the detail, see [14]).

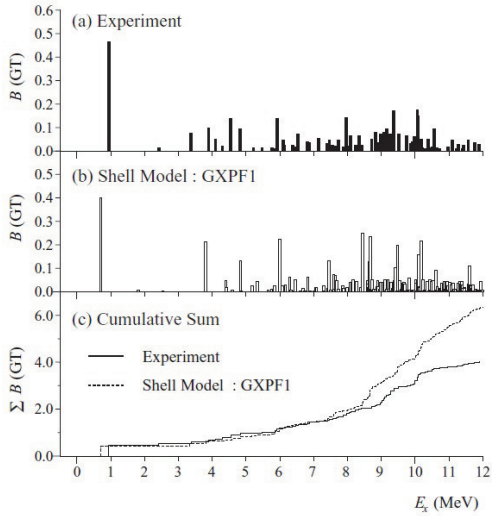

Fig. 3. Comparison of B(GT) strength distributions from the ^{54}Fe(^{3}He, t)^{54}Co measurement and a shell model (SM)calculation. (a) The experimental B(GT) distribution. (b) The B(GT) distribution obtained in the SM calculation using the GXPF1 interaction. (c) Cumulative sums of B(GT) values from the experiment and the SM calculation.

3. Study of $T_z = \pm 2 \rightarrow \pm 1$ mirror transitions

We have also been studying $T_z = \pm 2 \rightarrow \pm 1$ mirror GT transitions for the pf-shell nuclei. Starting from the 0^+ ground states of the $T_z = \pm 2$ even–even nuclei, the final $J^\pi = 1^+$ excited states in $T_z = \pm 1$ nuclei are reached in these transitions. The isospin symmetry of analog states and analogous $T_z = \pm 2 \rightarrow \pm 1$ GT and Fermi transitions in the "$T = 2$ isospin quintet" is shown schematically in Fig. 4 for the $A = 52$ and 56 systems.

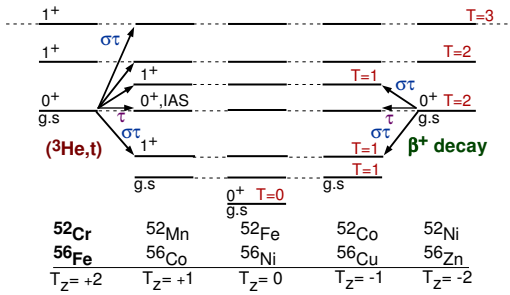

Fig. 4. (Color online) Schematic illustration of the "isospin symmetry" of GT transitions in the "$T = 2$ systems" with mass $A = 52$ and 56. The Coulomb displacement energies have been removed. The analogous $T_z = \pm 2 \rightarrow \pm 1$ transitions can be studied by the (^{3}He, t) reaction and β decay, respectively.

3.1. Mirror transitions in the $A = 52$ isospin quintet

In the $T_z = +2 \rightarrow +1$, ^{52}Cr(^{3}He, t)^{52}Mn experiment performed at RCNP, an energy resolution of $\Delta E = 29$ keV was achieved [see Fig. 5 (a)]. Since the proton separation energy of the final nucleus ^{52}Co is relatively low [$S_p = 1.58(4)$ MeV], the mirror ^{52}Ni $\rightarrow$ ^{52}Co β decay has been studied at GANIL by measuring the delayed-protons emitted from the final nucleus ^{52}Co [18]. The resolution of the proton measurement was about 150 keV (FWHM).

Starting from the (^{3}He, t) spectrum on ^{52}Cr, we can reconstruct the "β-decay spectrum" that is expected in the β decay of ^{52}Ni, the mirror nucleus of ^{52}Cr. Comparing Eqs. (1) and (3), we notice that the main difference is the f-factor in β decay that decreases drastically as a function of Q value (or excitation energy) [see Fig. 5 (b)]. By multiplying the f-factor of the ^{52}Ni β decay with the ^{52}Cr(^{3}He, t) spectrum shown in Fig. 5 (a), the spectrum given in Fig. 5 (c) is obtained. We see that the feedings to higher excited states are largely suppressed in β-decay studies.

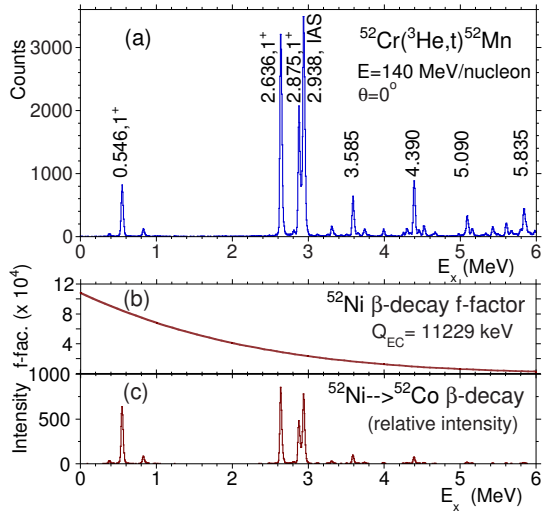

Fig. 5. (Color online) Derivation of a "β-decay spectrum" from the mirror (^{3}He, t) spectrum assuming isospin symmetry in the $A = 52$ isobar system. (a) The low-energy region of the ^{52}Cr(^{3}He, t)^{52}Mn spectrum for events with scattering angles $\Theta \leq 0.5°$. Major states with $\Delta L = 0$ are indicated by their (tentative) E_x values in MeV. (b) The f factor for the ^{52}Ni β decay. (c) The modified ^{52}Cr(^{3}He, t) spectrum obtained by multiplying the spectrum given in panel (a) with the f-factor shown in panel (b). Suppression of the feedings to higher excited states is expected in the β decay of the mirror nucleus ^{52}Ni.

By further correcting the difference of the coupling constants for the Fermi and GT transitions in the $(^3\mathrm{He}, t)$ reaction caused by the strong interaction and the β decay caused by the weak interaction, and also giving the width of 150 keV (FWHM) in the proton measurement, the spectrum one will expect to see in the ^{52}Ni β decay can be constructed. In order to make the correction for the coupling constants for the Fermi and GT transitions, it is important to have separation of them, and thus good separation of the IAS and nearby GT peaks. Therefore, high resolution was essential in the $(^3\mathrm{He}, t)$ reaction. More detail of the reconstruction of the "β-decay spectrum" is found in Ref. [19].

The delayed charged-particle spectrum from the ^{52}Ni β decay [18] is shown in Fig. 6 (a), while the "expected" β-decay spectrum is given in Fig. 6 (b). The solid line in the figure was obtained by a simple convolution

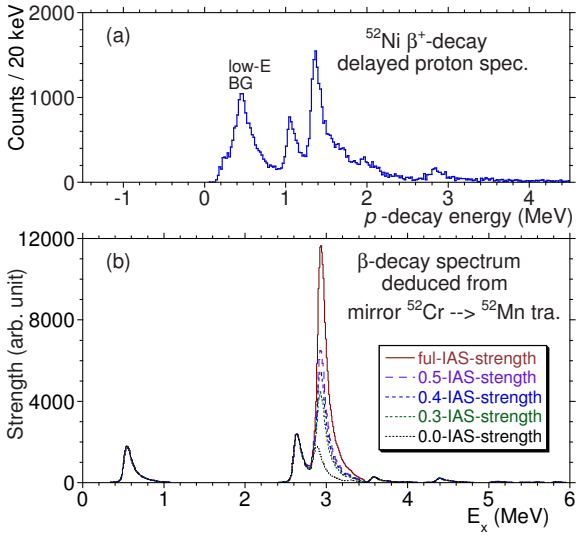

Fig. 6. (Color online) (a) The delayed charged-particle spectrum from the ^{52}Ni β decay [18]. The low-energy bump indicated by "low-E BG" originates in the emission of β^+ particles, while other peaks are from the delayed-proton emission, where the pileup with the β-particle energy broadens the peaks and makes the high-energy tails of the peaks wide. (b) The β-decay spectrum deduced from the $^{52}\mathrm{Cr}(^3\mathrm{He}, t)^{52}\mathrm{Mn}$ spectrum. First, the strength of the IAS peak was modified from the spectrum shown in Fig. 5 (c) to correct for the difference of the Fermi and GT coupling constants in the mirror β decay and CE reactions. Then, the spectrum was convoluted with the ΔE of 150 keV of the delayed-proton spectrum shown in panel (a). The inset shows the suppression factors of the IAS strength assumed in the simulations shown by the five different types of lines.

of the 150 keV width of the proton measurement. However, it is noted that the proton decay from the $T = 2$ IAS in ^{52}Co into a proton with $T = 1/2$ and $T = 1/2$ low-lying states in ^{51}Fe is not allowed by the isospin selection rule; the proton decay is possible only through the $T = 1$ isospin impurity of the IAS wave function and it is expected that the major part of the strength decays by γ transitions to the lower excited states in ^{52}Co. The dashed, short dashed, dotted and fine dotted lines in Fig. 6 (b) were obtained by reducing the IAS strength down to 0.5, 0.4, 0.3, and 0.0, respectively, in order to simulate the suppression of the proton decay. We see that there is a good agreement between the spectra shown in panels (a) and (b) when the suppression factor between 0.4 and 0.3 is assumed.

3.2. Mirror transitions in the A =56 isospin quintet

Since the proton separation energy of the daughter nucleus ^{56}Cu after the ^{56}Zn β decay is even lower [$S_p = 0.56(14)$ MeV], excited states populated in GT and Fermi transitions can be studied over a wide range in delayed-proton measurements. The mirror Fermi and GT transitions were studied in the ^{56}Fe(^{3}He, t)^{56}Co reaction. With a careful tuning of the beam and the use of a thin (≈ 1.1 mg/cm^2) target, an energy resolution of 19 keV (FWHM) was achieved [20]. With this excellent resolution, Fermi and near by GT states were clearly identified for the first time. On the basis of the analysis of the (^{3}He, t) reaction, the expected β-decay spectrum of the mirror nucleus ^{56}Zn was reconstructed assuming the isospin symmetry of the $T_z = \pm 2 \rightarrow \pm 1$ mirror GT transitions following the procedure described in Sec. 3.1 and is given in Fig. 7 (a). The measured proton spectrum from the daughter nucleus ^{56}Cu following the β decay of ^{56}Zn [21] is shown in Fig. 7 (b). In this β-decay experiment performed at GANIL, Caen, a resolution of 70 keV was achieved in the proton energy measurement using DSSSD detectors [22].

The full line of Fig. 7 (a) does not include the effect of the suppression of proton decay from the IAS by the isospin selection rule. In order to get a good agreement for both spectra in the IAS region ($E_x \approx 3.5$ MeV), a suppression factor of ≈ 0.3 is needed. This number is more or less in good agreement with the suppression factor of the IAS peak in the ^{52}Ni β decay discussed earlier in Sec. 3.1.

In a detailed comparison of Fig. 7 (a) and (b), we notice that there are qualitative differences between these spectra; in panel (b), we see two extra peaks, *i.e.*, the 1.391 MeV, 0^+ and 2.537 MeV, (1^+) states. Since the direct feeding of a 0^+ state other than the IAS is unusual in a β decay, it is suspected that the 1.391 MeV state was fed indirectly, and the same is true for the 2.537 MeV state.

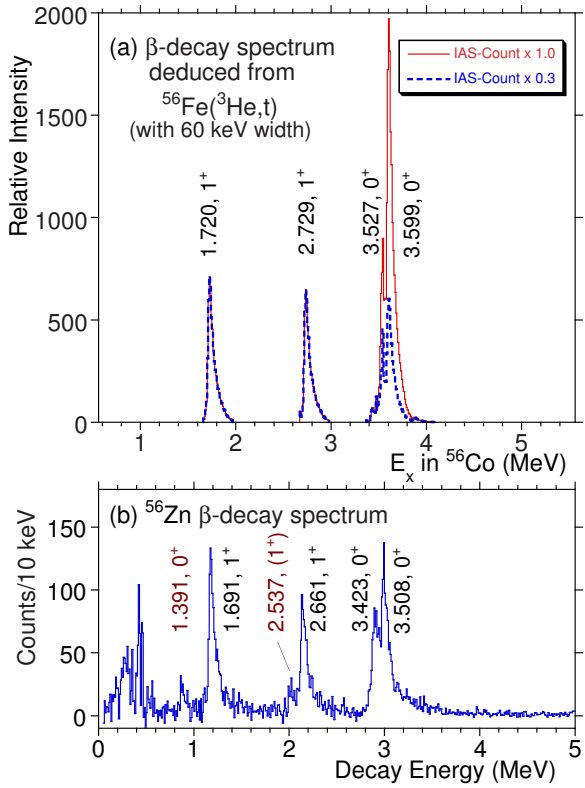

Fig. 7. (Color online) (a) The β-decay spectrum deduced from the ^{56}Fe(^{3}He, t)^{56}Co spectrum. The solid line was obtained by a simple convolution of the shape of the delayed-proton spectrum. The dashed lines were obtained by reducing the IAS strength down to 30% in order to simulate the suppression of the proton emission from the IAS. (b) The delayed proton spectrum from the ^{56}Zn β decay [21]. The low-energy bump originates in the emission of β^+ particles, while other peaks are from the proton emission.

Here, we should remember the fact that (1) the $S_p = 0.56$ MeV in the daughter nucleus ^{56}Cu is much lower than the $E_x = 3.51$ MeV of the IAS and (2) the proton decay from the $T = 2$ IAS in a $T_z = -1$ nucleus is isospin forbidden. Combining these two, we can conjecture that the two extra peaks are fed through the "β-delayed γ decay" of one of the 1^+ states or the IAS. Once fed, these states are allowed to make proton decays since these states are situated higher than the S_p value and they have $T = 1$. As described in detail in Ref. [21], the γ decay in coincidence with the ^{56}Zn β decay was studied and a decay scheme including the decay processes "β-delayed proton", "β-delayed γ", and "β-delayed γ-proton" was reconstructed.

As a result, we found that the delayed-proton spectrum does not always represents the branching ratio of the β decay of the mother nucleus; in other words the proton spectrum may be modified by the decay process "delayed-γ-proton". In order to understand and reconstruct the β-decay scheme of proton rich unstable nuclei far-from-stability, we found that the analysis including the results from $(^3\mathrm{He}, t)$ measurements on mirror nuclei is fruitful, where, with the high resolution of them, one can clearly separate states excited by Fermi and GT transitions.

4. Summary and prospects

Properties of GT transitions from proton rich unstable pf-shell nuclei are amongst the key ingredients required for an understanding of rp and other processes of nucleosynthesis. The β-decay studies of these unstable nuclei can, in principle, give absolute GT transition strength but only over a limited range of excitation energy determined by the Q value. On the other hand, the isospin analogous GT transitions that can be studied in detail using high-resolution $(^3\mathrm{He}, t)$ reactions give us an overview of GT strength distributions up to high excitation energies. Under the assumption of isospin symmetry, the analysis combining the information from both the β decay of unstable nuclei and the high-resolution study of the corresponding isospin analogous transitions provides a richer picture of a set of mass A isobars.

In addition, we find that the delayed-proton spectrum does not always represents the true branching ratios of the β decay of the mother nucleus because of the suppression of the delayed-proton decay from the IAS in the daughter nucleus. It should be noted that the exotic decay process "β-delayed γ-proton" can happen in a β decay from any nucleus far-from-stability with $T_z \leq -3/2$. In this respect, measurements of β-delayed γ rays are important even in the β-decay studies for proton rich unstable nuclei. This is an important message because such β-decay studies are planned at present and future radioactive beam facilities.

The high-resolution $(^3\mathrm{He}, t)$ experiments were performed at RCNP, Osaka, and the β-decay studies of $T_z = -1$ nuclei at GSI as a part of RISING campaign. The ^{56}Zn β-decay experiment was performed at GANIL, Caen. The authors are grateful to the participants in these experiments. This work was supported by MEXT, Japan under Grants No. 18540270 and No. 22540310; the Japan–Spain collaboration program by JSPS and CSIC; the Spanish MICINN under Grant No. EPA2008-06419-C02-01 and No. EPA2011-24553; CPAN Consolider-Ingenio 2010 Program CSD2007-00042; UK STFC Grant No. ST/F012012/1; and Region of Aquitaine.

REFERENCES

[1] F. Osterfeld, *Rev. Mod. Phys.* **64**, 491 (1992) and references therein.

[2] K. Langanke, G. Martínez-Pinedo, *Rev. Mod. Phys.* **75**, 819 (2003).

[3] Y. Fujita, B. Rubio, W. Gelletly, *Prog. Part. Nucl. Phys.* **66**, 549 (2011) and references therein.

[4] B. Rubio, W. Gelletly, *Lect. Notes Phys.* **764**, 99 (2009) and references therein.

[5] J.C. Hardy, I.S. Towner, *Phys. Rev.* **C79**, 055502 (2009) and references therein.

[6] J.C. Hardy, I.S. Towner, *Nucl. Phys. News* **16**, 11 (2006).

[7] T.N. Taddeucci *et al.*, *Nucl. Phys.* **A469**, 125 (1987).

[8] Y. Fujita *et al.*, *Phys. Rev.* **C67**, 064312 (2003).

[9] Y. Fujita *et al.*, *Phys. Rev.* **C59**, 90 (1999).

[10] See web site `http://www.rcnp.osaka-u.ac.jp`

[11] Y. Fujita *et al.*, *Phys. Rev. Lett.* **112**, 112502 (2014).

[12] T. Adachi *et al.*, *Phys. Rev.* **C73**, 024311 (2006).

[13] Y. Fujita *et al.*, *Phys. Rev. Lett.* **95**, 212501 (2005).

[14] T. Adachi *et al.*, *Phys. Rev.* **C85**, 024308 (2012).

[15] H. Fujita *et al.*, *Phys. Rev.* **C75**, 034310 (2007).

[16] F. Molina *et al.*, *Phys. Rev.* **C91**, 014301 (2015).

[17] M. Honma *et al.*, *Phys. Rev.* **C69**, 034335 (2004).

[18] C. Dossat *et al.*, *Nucl. Phys.* **A792**, 18 (2007).

[19] Y. Fujita *et al.*, *Phys. Rev.* **C88**, 014308 (2013).

[20] H. Fujita *et al.*, *Phys. Rev.* **C88**, 054329 (2013).

[21] S.E.A. Orrigo *et al.*, *Phys. Rev. Lett.* **112**, 222501 (2014).

[22] S.E.A. Orrigo *et al.*, *Acta Phys. Pol. B* **46**, 709 (2015), this issue.